CIPM MRA
Comparison reports

BIPM.RI(I)-K7 (ENEA-INMRI 2025)

Measurement of air kerma for mammography beams

KEY COMPARISON

Any further distribution of this Report must be cited as:
A. Villevalde *et al* 2026 *CIPM MRA Comparison reports* **06010**

https://doi.org/10.59161/LWJC9046

Key comparison BIPM.RI(I)-K7 of the air-kerma standards of the ENEA-INMRI, Italy, and the BIPM in mammography x-rays

A Villevalde[1], C Kessler[1], F Curciarello[2], G Cappadozzi[2], A Ciccotelli[2], C Silvestri[2], M Pinto[2]

[1] Bureau International des Poids et Mesures, Pavillon de Breteuil, F-92312 Sèvres CEDEX
[2] ENEA-Istituto Nazionale di Metrologia delle Radiazioni Ionizzanti,
C.R. Casaccia, c.p. 00123 Rome, Italy

Abstract A new key comparison has been made between the air-kerma standards of the ENEA-INMRI, Italy, and the BIPM in mammography x-ray beams. The results show the standards to agree at the level of the expanded uncertainty of the comparison of 7.8 parts in 10^3. The results are analysed and presented in terms of degrees of equivalence, suitable for entry in the BIPM key comparison database.

1. Introduction

An indirect comparison has been made between the air-kerma standards of the Istituto Nazionale di Metrologia delle Radiazioni Ionizzanti (INMRI) of the Agenzia Nazionale per le Nuove Tecnologie, l'Energia e lo Sviluppo Economico Sostenibile (ENEA), Italy, and the Bureau International des Poids et Mesures (BIPM) in mammography x-ray beams in the range from 23 kV to 35 kV to update the previous comparison result of 2014 (Kessler *et al*. 2015) published in the BIPM key comparison database (KCDB 2026) under the reference BIPM.RI(I)-K7. Measurements were done in the set of mammography qualities using the tungsten-anode x-ray tube with molybdenum filtration (W/Mo radiation beams). Three thin-window parallel-plate ionization chambers were used as transfer instruments. The measurements at the BIPM took place in March 2025 using the reference conditions recommended by the CCRI as described in Kessler and Burns (2024). Final data for the evaluation of the comparison results were received from the ENEA-INMRI in June 2025 and the final version of the report in April 2026.

2. Determination of the air-kerma rate

For a free-air ionization chamber standard with measuring volume V, the air-kerma rate is determined by the relation

$$\dot{K} = \frac{I}{\rho_{\mathrm{air}} V} \frac{W_{\mathrm{air}}}{e} \frac{1}{1 - g_{\mathrm{air}}} \prod_i k_i \tag{1}$$

where ρ_{air} is the density of air under reference conditions, I is the ionization current under the same conditions, W_{air} is the mean energy expended by an electron of charge e to produce an ion pair in air, g_{air} is the fraction of the initial electron energy lost through radiative processes in air, and $\Pi\, k_i$ is the product of the correction factors to be applied to the standard.

The value used for ρ_{air} at both laboratories is given in Table 1. For use with this dry-air value, the ionization current measured for the standard must be corrected for humidity and for the difference between the density of the air of the measuring volume at the time of measurement and the value given in the table[1]. The value used for W_{air}/e is that recommended in ICRU Report 90 (ICRU 2016) for dry air, also given in Table 1.

[1] For an air temperature $T \sim 293$ K, pressure P and relative humidity ~50 % in the measuring volume, the correction for air density for the standard involves a temperature correction T / T_0, a pressure correction P_0 / P and a humidity correction $k_h = 0.9980$.

3. Details of the standards

Both free-air chamber standards are of the conventional parallel-plate design. The BIPM air-kerma standard is described in Boutillon *et al.* (1969) and Kessler (2006) and the changes made to certain correction factors are given in Burns (2004), Burns and Kessler (2009) and Burns *et al.* (2009). Implementation of the recommendations of ICRU Report 90 (ICRU 2016) is reported in Burns and Kessler (2018). The ENEA-INMRI standard is described in the report of the previous comparison with the BIPM (Kessler *et al.* 2015), and the changes made to certain correction factors are given in Laitano *et al.* (2005). The changes made following ICRU Report 90 (ICRU 2016) were implemented in April 2021 and reported to the CCRI(I) at the meeting in June 2021. The main dimensions, the measuring volume and the polarizing voltage for each standard are shown in Table 2.

Table 1. Physical constants used in the determination of the air-kerma rate

Constant	Value	u_i [a]
ρ_{air} [b]	1.2045 kg m^{-3}	0.0001
W_{air} / e	33.97 J C^{-1}	0.0035

[a] u_i is the relative standard uncertainty.
[b] Density of dry air at T_0 = 293.15 K and P_0 = 101.325 kPa adopted at the BIPM and at the ENEA-INMRI.

Table 2. Main characteristics of the standards

Standard	BIPM L-01	ENEA-INMRI
Aperture diameter / mm	9.941	8.014
Air path length / mm	100.0	65.12
Collecting length / mm	15.466	40.738
Electrode separation / mm	70	60
Collector width / mm	71	60
Measuring volume / mm^3	1200.4	2054.9
Polarizing voltage / V	1500	1600

4. The transfer instruments

4.1 Determination of the calibration coefficient for a transfer instrument

The air-kerma calibration coefficient N_K for a transfer instrument is given by the relation

$$N_K = \frac{\dot{K}}{I_{\mathrm{tr}}} \tag{2}$$

where $\dot{K}$ is the air-kerma rate determined by the standard using Equation (1) and I_{tr} is the ionization current measured by the transfer instrument and the associated current-measuring system. The current I_{tr} is corrected to the standard conditions of air temperature, pressure and relative humidity chosen for the comparison (T = 293.15 K, P = 101.325 kPa, RH = 50 %). No humidity correction is applied to the current measured using transfer instruments, on the basis that the BIPM laboratory is maintained with a relative humidity in the range from 40 % to 55 % and the ENEA-INMRI laboratory remained in the range from 45 % to 55 %.

To derive a comparison result from the calibration coefficients $N_{K,\mathrm{BIPM}}$ and $N_{K,\mathrm{NMI}}$ measured, respectively, at the BIPM and at a national metrology institute (NMI), differences in the radiation qualities must be taken into account. Normally, each quality used for the comparison has the same nominal generating potential and similar filtration at each institute, but the half-value layers (HVLs) can differ appreciably. A radiation quality correction factor k_Q is derived for each comparison quality Q. This corrects the calibration coefficient $N_{K,\mathrm{NMI}}$ determined at the NMI into one that applies at the 'equivalent' BIPM quality and is derived from a fit to the $N_{K,\mathrm{NMI}}$ values in terms of log(HVL). The comparison result at each quality is then taken as

$$R_K = \frac{k_Q N_{K,\mathrm{NMI}}}{N_{K,\mathrm{BIPM}}}\,. \tag{3}$$

In practice, the half-value layers normally differ by only a small amount and k_Q is close to unity. For the present comparison, this is discussed in section 7.2.

4.2 Details of the transfer instruments

Three thin-window parallel-plate ionization chambers belonging to the ENEA-INMRI, two of type Radcal RC6M, serial numbers 10206 and 10279, and one type Exradin Magna A650, serial number D222221, were used as transfer instruments for the comparison. Their main characteristics are given in Table 3. For positioning the chambers at the reference distance, the red line around the casing of Radcal chambers (measured 8.4 mm and 8.3 mm from the front of the casing for 10206 and 10279 chambers, respectively) was positioned in the reference plane. Similarly, the black line engraved around the casing of the Exradin Magna A650 chamber (4.0 mm from the front of the casing) was positioned in the reference plane.

Table 3. Main characteristics of the transfer chambers

Chamber type	Radcal RC6M	Exradin Magna A650
Window material	metallized polyester	Kapton
Window thickness / mg cm^{-2}	0.7	3.86
Nominal volume / cm^3	6	3.46
Collector diameter / mm	30 [a]	21.9
Cavity height / mm	8 [a]	7.95
External diameter / mm	43.8	53.4
Polarizing potential [b] / V	300	300

[a] The Radcal RC6M cavity dimensions are not clearly stated by the manufacturer. From radiographic measurements, the collector diameter is known to be close to 30 mm, and ionometric measurements indicate a cavity volume of about 5.8 cm^3, consistent with the value 6 cm^3 stated by the manufacturer. From these, the cavity height is deduced to be around 8.2 mm, which would position the collector close to the red line around the chamber casing.

[b] At both laboratories, a positive polarizing potential was applied to the chamber window.

5. Calibration at the BIPM

5.1 The BIPM irradiation facility and reference radiation qualities

The BIPM low-energy x-ray laboratory houses a high-stability generator and a tungsten-anode x-ray tube with an inherent filtration of 1 mm beryllium. A voltage divider is used to measure the generating potential, which is stabilized using an additional feedback system of the BIPM. Rather than using a transmission monitor, which might introduce its own variability, the anode current is measured, and the ionization chamber current is normalized for any deviation from the reference anode current. The standard deviation of repeat air-kerma rate determinations over many months is typically 3 parts in 10^4. The radiation qualities used in the range from 23 kV to 35 kV are those recommended by the CCRI and are given in Table 4 in ascending HVL from left to right.

Note that for the present comparison the ENEA-INMRI used the reference distance of 500 mm from the radiation source for the calibration of the Radcal RC6M chambers and 1000 mm from the radiation source for the calibration of the Exradin Magna A650 chamber and so the BIPM measurements were also made at the mentioned distances.

The irradiation area is temperature controlled at around 20 °C and is stable over the duration of a calibration to better than 0.1 °C. Two calibrated thermistors measure the temperature of the ambient air and the air inside the BIPM standard. Air pressure is measured by means of a calibrated barometer.

Table 4. Characteristics of the BIPM reference radiation qualities used for the ENEA-INMRI comparison

Radiation quality	W/Mo 23	W/Mo 28	W/Mo 30	W/Mo 35
Generating potential / kV	23	28	30	35
Additional filtration	60 µm Mo			
Al HVL / mm (0.5 m)	0.332	0.355	0.364	0.388
Al HVL [a] / mm (1 m)	0.343	0.368	0.377	0.403
$(\mu/\rho)_{air}$ [b] / cm^2 g^{-1} (0.5 m)	1.79	1.70	1.67	1.60
$(\mu/\rho)_{air}$ [a, b] / cm^2 g^{-1} (1 m)	1.74	1.63	1.61	1.54
$\dot{K}_{\mathrm{BIPM}}$ / mGy s^{-1} (0.5 m)	1.00	1.00	1.00	1.00
$\dot{K}_{\mathrm{BIPM}}$ / mGy s^{-1} (1 m)	0.23	0.23	0.23	0.24

[a] Measured at 1 m as described by Villevalde *et al.* (2020).
[b] Measured for an equivalent air-path length of 100 mm using a variable-pressure tube.

5.2 BIPM standards and correction factors

As mentioned above, for the present comparison the reference plane for the BIPM standard was positioned at 500 mm and at 1000 mm from the exit window of the x-ray tube for the calibration of the Radcal RC6M chambers and the Exradin Magna A650 chamber, respectively, with a reproducibility of 0.03 mm. The standard was aligned on the beam axis to an estimated uncertainty of 0.1 mm. For these measurements, an additional tungsten collimator was used to give a beam diameter of around 50 mm at the reference distance of 500 mm and around 100 mm at the reference distance of 1000 mm for all radiation qualities, to reproduce the ENEA-INMRI measurement conditions.

For the calibration of transfer chambers, measurements using the BIPM standard were made using positive polarity only. A correction factor of 1.0005 is applied to correct for the known polarity effect in the standard (see Table 5). The leakage current for the BIPM standard, relative to the ionization current, was measured to be less than 1 part in 10^4.

The correction factors applied to the ionization current measured at each radiation quality using the BIPM standard, together with their associated standard uncertainties, are given in Table 5.

Table 5. Correction factors and uncertainties for the BIPM standard

Radiation quality	W/Mo 23	W/Mo 28	W/Mo 30	W/Mo 35	$u_{i\mathrm{A}}$	$u_{i\mathrm{B}}$
Air attenuation k_a [a] (0.5 m)	1.0218	1.0208	1.0203	1.0195	0.0002	0.0001
Air attenuation k_a [a] (1 m)	1.0212	1.0198	1.0196	1.0188	0.0002	0.0001
Photon scatter k_{sc}	0.9974	0.9974	0.9974	0.9974	-	0.0003
Fluorescence k_{fl}	0.9972	0.9972	0.9972	0.9973	-	0.0005
Electron loss k_e	1.0000	1.0000	1.0000	1.0000	-	0.0001
Initial ionization k_{ii} [b] Energy dependence of W_{air} k_W [b]	0.9970	0.9971	0.9971	0.9972	-	0.0012
Ion recombination k_s (0.5 m)	1.0007	1.0007	1.0007	1.0007	0.0001	0.0001
Ion recombination k_s (1 m)	1.0004	1.0004	1.0004	1.0004	0.0001	0.0001
Polarity k_{pol}	1.0005	1.0005	1.0005	1.0005	0.0001	-
Field distortion k_d	1.0000	1.0000	1.0000	1.0000	-	0.0007
Diaphragm effects k_{dia}	0.9996	0.9996	0.9996	0.9996	-	0.0003
Wall transmission k_p	1.0000	1.0000	1.0000	1.0000	0.0001	-
Humidity k_h	0.9980	0.9980	0.9980	0.9980	-	0.0003
$1 - g_{air}$	1.0000	1.0000	1.0000	1.0000	-	0.0001

[a] Values for 293.15 K and 101.325 kPa; each measurement is corrected using the air density measured at the time.
[b] The stated values are for the product $k_{ii}k_W$, as presented in Burns and Kessler (2018).

The largest correction is that due to the attenuation of the x-ray fluence along the air path between the reference plane and the centre of the collecting volume. The corresponding correction factor k_a is evaluated using the measured mass attenuation coefficients for air $(\mu/\rho)_{air}$ given in Table 4 for both distances. In practice, the values used for k_a take account of the temperature and pressure of the air in the standard.

5.3 Transfer chamber positioning and calibration at the BIPM

The reference point for each chamber was positioned in the reference plane with a reproducibility of 0.03 mm. Each transfer chamber was aligned laterally on the beam axis to an estimated uncertainty of 0.1 mm. The leakage current was measured before and after each series of ionization current measurements and a correction made using the mean value. The leakage current relative to the ionization current for each chamber was less than 1 part in 10^4.

The calibration procedure involves measurements with the transfer chamber and with the standard at a given radiation quality before proceeding to the next quality, with a period of typically 10 minutes following a change of quality to allow the generator and tube to stabilize. For each of the transfer chambers at each radiation quality, the relative standard uncertainty of the mean ionization current was about 2 parts in 10^4. Based on the results of repeat calibrations including chamber repositioning and on long-term experience of calibrations in these beams, an uncertainty component of 5 parts in 10^4 is included in Table 12 for the short-term reproducibility of the calibration coefficients determined at the BIPM.

6. Calibration at the ENEA-INMRI

6.1 ENEA-INMRI irradiation facility and reference radiation qualities

The mammography x-ray facility at the ENEA-INMRI uses a constant-potential generator and tungsten-anode tube and an inherent filtration of 0.8 mm beryllium. The x-ray output is monitored by means of a free-air, custom-made monitor ionization chamber. The standard deviation of repeated determinations of the air-kerma rate at either 500 mm or 1000 mm distance from the radiation source, on average across all qualities, over the period of a transfer chamber calibration, is less than 3 parts in 10^3. The generating potential is measured invasively with a voltage divider.

To determine the chamber calibration coefficient, sequential measurements were carried out using the primary standard and the transfer ionization chamber, without applying monitor chamber normalization.

The characteristics of the ENEA-INMRI radiation qualities are given in Table 6.

The irradiation area is temperature controlled around 20 °C and is stable over the duration of a calibration to better than 0.5 °C. Two calibrated NTC type thermometers are used to measure air temperature, one positioned either inside the primary standard or near the transfer chamber under calibration, and the second located near the monitor chamber. The air pressure is measured using a calibrated barometer whose probe is positioned at approximately the same height as the beam central axis.

Table 6. Characteristics of the ENEA-INMRI reference radiation qualities

Radiation quality	W/Mo 23	W/Mo 28	W/Mo 30	W/Mo 35
Generating potential / kV	23	28	30	35
Additional filtration	60 µm Mo			
Al HVL / mm (0.5 m)	0.323	0.346	0.349	0.382
Al HVL / mm (1 m)	0.335	0.360	0.368	0.394
$(\mu/\rho)_{\mathrm{air}}$ [a] / cm^2 g^{-1} (0.5 m)	1.73	1.68	1.66	1.49
$(\mu/\rho)_{\mathrm{air}}$ [a] / cm^2 g^{-1} (1 m)	1.63	1.56	1.56	1.47
$\dot{K}_{\text{ENEA-INMRI}}$ / mGy s^{-1} (0.5 m)	1.73	2.64	2.99	3.85
$\dot{K}_{\text{ENEA-INMRI}}$ / mGy s^{-1}(1 m)	0.51	0.62	0.70	0.91

[a] Measured using a variable-pressure tube. The determination of the mass attenuation coefficient relies on a correction to account for the attenuation effects of the two 0.5 mm beryllium windows that act as walls of the tube.

6.2 ENEA-INMRI standard and correction factors

At the ENEA-INMRI, the reference distance is 500 mm from the exit window of the x-ray tube, with a beam diameter of 50 mm. The Radcal chambers were calibrated using these reference conditions. However, the calibration of the Exradin Magna A650 chamber, due to its larger external diameter, was performed at 1000 mm from the exit window of the x-ray tube, where the beam diameter is 100 mm. The reference plane for the ENEA-INMRI standard was positioned at the mentioned distances with an uncertainty of about 0.1 mm and 1 mm, respectively. The standard was aligned laterally on the beam axis with an estimated uncertainty of about 0.2 mm.

During the calibration of the transfer chambers, measurements using the ENEA-INMRI standard were made using positive polarity only. A correction factor included in Table 7 is applied to correct for the known polarity effect in the standard. The leakage current for the ENEA-INMRI standard was below 0.5 pA (worst case), corresponding to less than 1 part in 10^3, relative to the ionization current.

The correction factors applied to the ionization current measured at each radiation quality using the ENEA-INMRI standard, together with their associated uncertainties, are given in Table 7.

Table 7. Correction factors and uncertainties for the ENEA-INMRI standard

Radiation quality	W/Mo 23	W/Mo 28	W/Mo 30	W/Mo 35	$u_{i\mathrm{A}}$	$u_{i\mathrm{B}}$
Air attenuation k_a [a] (0.5 m)	1.0137	1.0133	1.0131	1.0118	0.0002	0.0010
Air attenuation k_a [a] (1 m)	1.0129	1.0123	1.0123	1.0116	0.0002	0.0010
Scattered radiation k_{sc}	0.9983	0.9983	0.9983	0.9983	-	0.0006
Fluorescence k_{fl}	0.9978	0.9979	0.9979	0.9979	-	0.0006
Electron loss k_e	1.0000	1.0000	1.0000	1.0000	-	0.0002
Initial ionization k_{ii} [b] Energy dependence of W_{air} k_W [b]	0.9971	0.9971	0.9971	0.9972	-	0.0012
Ion recombination k_s (0.5 m)	1.0007	1.0008	1.0009	1.0010	-	0.0005
Ion recombination k_s (1 m)	1.0005	1.0005	1.0005	1.0006	-	0.0005
Polarity k_{pol}	0.9999	0.9999	0.9999	0.9999	-	0.0006
Field distortion k_d	1.0000	1.0000	1.0000	1.0000	-	0.0010
Aperture transmission k_l	0.9997	0.9997	0.9997	0.9996	-	0.0004
Wall transmission k_p	1.0000	1.0000	1.0000	1.0000	-	0.0005
Humidity k_h [c]	0.9980	0.9980	0.9980	0.9980	-	0.0003
$1 - g_{air}$	1.0000	1.0000	1.0000	1.0000	-	0.0001

[a] Values for 293.15 K and 101.325 kPa; each measurement is corrected using the air density measured at the time.

[b] The stated values are for the product $k_{ii}k_W$ implemented according to ICRU Report 90 (ICRU 2016).

[c] Each measurement is corrected using the relative partial vapor pressure calculated at the time of measurement according to ICRU Report 31 (ICRU 1979).

The correction factors k_a are evaluated using the measured mass attenuation coefficients for air given in Table 6. In practice, the values used for k_a take account of the temperature and pressure of the air in the standard at the time of the measurements.

6.3 Transfer chamber positioning and calibration at the ENEA-INMRI

The reference point of the transfer chamber was positioned at 500 mm from the exit window of the x-ray tube for the Radcal RC6M chambers and at 1000 mm from the exit window of the x-ray tube for the Exradin Magna A650 chamber, with an uncertainty of around 0.1 mm and 1 mm, respectively. Each transfer chamber was aligned laterally on the beam axis to an estimated uncertainty of 0.2 mm. The leakage current was measured for each measurement series and a correction applied. The leakage current was typically below 0.2 pA (worst case), corresponding to less than 5 parts in 10^4, relative to the ionization current.

For each transfer chamber at each radiation quality, four calibrations were made before the measurements at the BIPM and one following the return of the chambers to the ENEA-INMRI. The uncertainty arising from these repeat measurements is discussed in Section 8.

7. Additional considerations for transfer chamber calibrations

7.1 Ion recombination, polarity, radial non-uniformity, distance and field size

Ion recombination: As can be seen from Tables 4 and 6, the ENEA-INMRI and BIPM air-kerma rates differ for both reference distances. The ENEA-INMRI applies a correction for ion recombination $k_{s,tr}$ calculated for each radiation quality as

$$k_{s,tr} = 1 + k_{init} + k_{vol} \times I \qquad (4)$$

where k_{init} is the initial recombination and k_{vol} is the volume recombination determined using the Niatel method (Boutillon 1998). The values determined at the ENEA-INMRI for both transfer chamber types are given in Table 8.

For consistency, the BIPM results have been corrected by $k_{s,tr}$ using the ENEA-INMRI determination and a corresponding uncertainty for ion recombination of 5 parts in 10^4 is included in Table 13.

Table 8. Ion recombination for the transfer chambers determined at the ENEA-INMRI

Coefficient	Radcal RC6M	Exradin Magna A650
Initial recombination, k_{init}	0.00196	0.00032
Volume recombination, k_{vol} / C^{-1}	6.68×10^5	3.92×10^5

Polarity: Each transfer chamber was used with the same polarity at each laboratory and so no correction is applied for the polarity effect.

Radial non-uniformity: The ENEA-INMRI correction for the radial non-uniformity of the beam was determined from measured beam profiles at the reference distances of 500 mm and 1000 mm. The correction for finite chamber dimensions was taken into account according to Kondo and Randolph (1960) and Bielajew (1990). For the Radcal RC6M chambers with a collector diameter of 30 mm, the resulting correction at 500 mm is 1.0021(11). For the Exradin Magna A650 chamber, with a collector diameter of 21.9 mm, the correction at 1000 mm is 1.0009(11). A similar correction was calculated for the BIPM beams. No correction $k_{rn,tr}$ is applied at either laboratory for the radial non-uniformity of the radiation field and a relative standard uncertainty of 1 part in 10^3 is included in Table 13.

Distance: As the chambers were calibrated at the BIPM at the same distances as the ENEA-INMRI (500 mm and 1000 mm for the Radcal RC6M and Exradin Magna A650 chambers, respectively), no correction for the distance effect was applied.

Field size: No correction is applied for field size as the BIPM field diameter was adjusted to match the ENEA-INMRI field size.

7.2 Radiation quality correction factors k_Q

As noted in Section 4.1, slight differences in the realizations of the CCRI radiation qualities at the ENEA-INMRI and the BIPM might require a correction factor k_Q. For the Radcal RC6M chambers, the correction factors k_Q were taken to be unity for all qualities, as the calculated factors were less than 2 parts in 10^4. For the Exradin Magna A650 chamber, the k_Q values given in Table 9 were applied. A relative standard uncertainty of 2 parts in 10^4 is included in Table 13.

8. Comparison results

The calibration coefficients $N_{K,\text{ENEA-INMRI}}$ and $N_{K,\text{BIPM}}$ for the transfer chambers are presented in Table 9.

Table 9. Calibration coefficients for the transfer chambers

Radiation quality	W/Mo 23	W/Mo 28	W/Mo 30	W/Mo 35
Radcal RC6M-10206				
$N_{K,\text{ENEA-INMRI}}$ (pre-BIPM) / Gy µC^{-1}	4.593	4.593	4.592	4.591
$N_{K,\text{ENEA-INMRI}}$ (post-BIPM) / Gy µC^{-1}	4.585	4.588	4.589	4.589
$s_{\text{stab},1}$	0.0016	0.0010	0.0006	0.0004
k_Q for $N_{K,\text{ENEA-INMRI}}$	1.0000	1.0000	1.0000	1.0000
$N_{K,\text{BIPM}}$ / Gy µC^{-1}	4.615	4.618	4.617	4.620
Radcal RC6M-10279				
$N_{K,\text{ENEA-INMRI}}$ (pre-BIPM) / Gy µC^{-1}	4.661	4.663	4.661	4.663
$N_{K,\text{ENEA-INMRI}}$ (post-BIPM) / Gy µC^{-1}	4.665	4.662	4.658	4.654
$s_{\text{stab},2}$	0.0008	0.0002	0.0006	0.0018
k_Q for $N_{K,\text{ENEA-INMRI}}$	1.0000	1.0000	1.0000	1.0000
$N_{K,\text{BIPM}}$ / Gy µC^{-1}	4.700	4.698	4.699	4.702
Exradin Magna A650-D222221				
$N_{K,\text{ENEA-INMRI}}$ (pre-BIPM) / Gy µC^{-1}	8.234	8.221	8.218	8.200
$N_{K,\text{ENEA-INMRI}}$ (post-BIPM) / Gy µC^{-1}	8.265	8.241	8.240	8.221
$s_{\text{stab},3}$	0.0035	0.0022	0.0025	0.0024
k_Q for $N_{K,\text{ENEA-INMRI}}$	0.9993	0.9994	0.9993	0.9993
$N_{K,\text{BIPM}}$ / Gy µC^{-1}	8.295	8.283	8.278	8.268

For each chamber at each radiation quality, the values $N_{K,\text{ENEA-INMRI}}$ provided before and after the measurements at the BIPM give rise to the mean value used for the final comparison result and a relative standard uncertainty s_{stab} representing the chamber stability[2].

The comparison results R_K are presented in Table 10, evaluated according to Equation (3). For each radiation quality the final comparison result is evaluated as the mean for the three transfer chambers. The uncertainty s_{tr} is the standard uncertainty of this mean, or taken as

$$s_{\text{tr}} = \frac{\sqrt{s_{\text{stab},1}^2 + s_{\text{stab},2}^2 + s_{\text{stab},3}^2}}{3} \tag{5}$$

if this is larger (on the basis that the agreement between the comparison results for different transfer chambers should not, on average, be better than their combined stability estimated using $s_{\text{stab},1}$, $s_{\text{stab},2}$ and $s_{\text{stab},3}$ from Table 9). The root mean squared (rms) value of s_{tr} for the four qualities, $s_{\text{tr,comp}} = 0.0011$, is taken to represent the uncertainty arising from the transfer chambers and is included in Table 13.

Also given in the final row of Table 10 are the results for the ENEA-INMRI in the previous comparison in 2014, revised for the changes made to the standards at each laboratory.

Table 10. Combined comparison results

Radiation quality	W/Mo 23	W/Mo 28	W/Mo 30	W/Mo 35
R_K using Radcal RC6M-10206	0.9944	0.9940	0.9943	0.9935
R_K using Radcal RC6M-10279	0.9921	0.9924	0.9916	0.9907
R_K using Exradin Magna A650-D222221	0.9938	0.9931	0.9934	0.9924
s_{tr}	0.0013	0.0008	0.0009	0.0010
Final R_K	**0.9934**	**0.9932**	**0.9931**	**0.9922**
Updated 2014 results using Radcal RC6M-10206	0.9964	0.9968	0.9971	0.9968

9. Uncertainties

The uncertainties associated with the primary standards are listed in Table 11, and those for the transfer chamber calibrations in Table 12. The combined standard uncertainty u_c for the comparison results R_K is presented in Table 13.

The combined standard uncertainty of the comparison result takes into account correlation in the type B uncertainties associated with the physical constants, the humidity correction and the factor $k_{\text{ii}}k_W$. Correlation in the values for k_{e}, k_{l}, k_{sc} and k_{fl}, derived from Monte Carlo calculations in each laboratory, are taken into account in an approximate way by assuming half of the uncertainty value for each factor at each laboratory. This is consistent with the analysis of the results of BIPM comparisons in low-energy x-rays in terms of degrees of equivalence described in Burns (2003).

[2] Because of the very small sample size, the modified standard uncertainty including the appropriate t-factor is used, which for $n = 2$ gives $s_{\text{stab}} = 1.8\, s_{\text{dev.s}}/\sqrt{2}$. Likewise for s_{tr}.

10. Discussion

The comparison results presented in Table 10 show general agreement at the level of the expanded uncertainty for the comparison of 7.8 parts in 10^3.

No trend is observed in the results for the different radiation qualities. While the use of transfer chambers might introduce more uncertainty in the comparison results than for a direct comparison of the primary standards, useful information is gained on the reproducibility of calibration coefficients.

Table 11. Uncertainties associated with the standards

Standard	BIPM L-01		ENEA-INMRI	
Relative standard uncertainty	$u_{i\mathrm{A}}$	$u_{i\mathrm{B}}$	$u_{i\mathrm{A}}$	$u_{i\mathrm{B}}$
Ionization current	0.0002	0.0002	0.0005	0.0016
Air density correction	-	-	0.0002	0.0004
Leakage	-	-	-	0.0005
Positioning	0.0001	0.0001	-	0.0002
Volume	0.0003	0.0005	-	0.0005
Correction factors (excl. k_h)	0.0003	0.0015	0.0002	0.0023
Humidity k_h	-	0.0003	-	0.0003
Physical constants	-	0.0035	-	0.0035
$\dot{K}$	0.0005	0.0039	0.0006	0.0046

Table 12. Uncertainties associated with the calibration of the transfer chambers

Institute	BIPM		ENEA-INMRI	
Relative standard uncertainty	$u_{i\mathrm{A}}$	$u_{i\mathrm{B}}$	$u_{i\mathrm{A}}$	$u_{i\mathrm{B}}$
$\dot{K}$	0.0005	0.0039	0.0006	0.0046
I_tr	0.0002	0.0002	0.0010	0.0016
Humidity	-	-	-	0.0003
Positioning of transfer chamber	0.0001	-	-	0.0010
Reproducibility	0.0005	-	0.0020	-
N_K	0.0007	0.0039	0.0023	0.0050

Table 13. Uncertainties associated with the comparison results

Relative standard uncertainty	$u_{i\mathrm{A}}$	$u_{i\mathrm{B}}$
$N_{K,\mathrm{ENEA\text{-}INMRI}}$ / $N_{K,\mathrm{BIPM}}$	0.0024	0.0027 [a]
Ion recombination	-	0.0005
Radial non-uniformity	-	0.0010
k_Q	-	0.0002
Transfer chambers $s_{\mathrm{tr,comp}}$	0.0011	-
R_K	0.0026	0.0029 [a]
	u_c = 0.0039 [a]	

[a] Takes account of correlation in type B uncertainties.

The results agree with the results of the indirect comparison carried out in 2014 at the level of the expanded standard uncertainty of the comparisons.

The 2014 comparison results are shown in Table 10; the comparison was done using the Radcal RC6M chamber, serial number 10206. The present BIPM calibration coefficients for this chamber have increased by 1.0018(4) when comparing with the 2014 results, keeping the same energy dependence. The 2025 ENEA-INMRI results show a change with energy, where the 2025 results are lower than the previous ones, by 0.9993 at 23 kV and decreasing to 0.9982 at 35 kV. The results are shown in Figure 1.

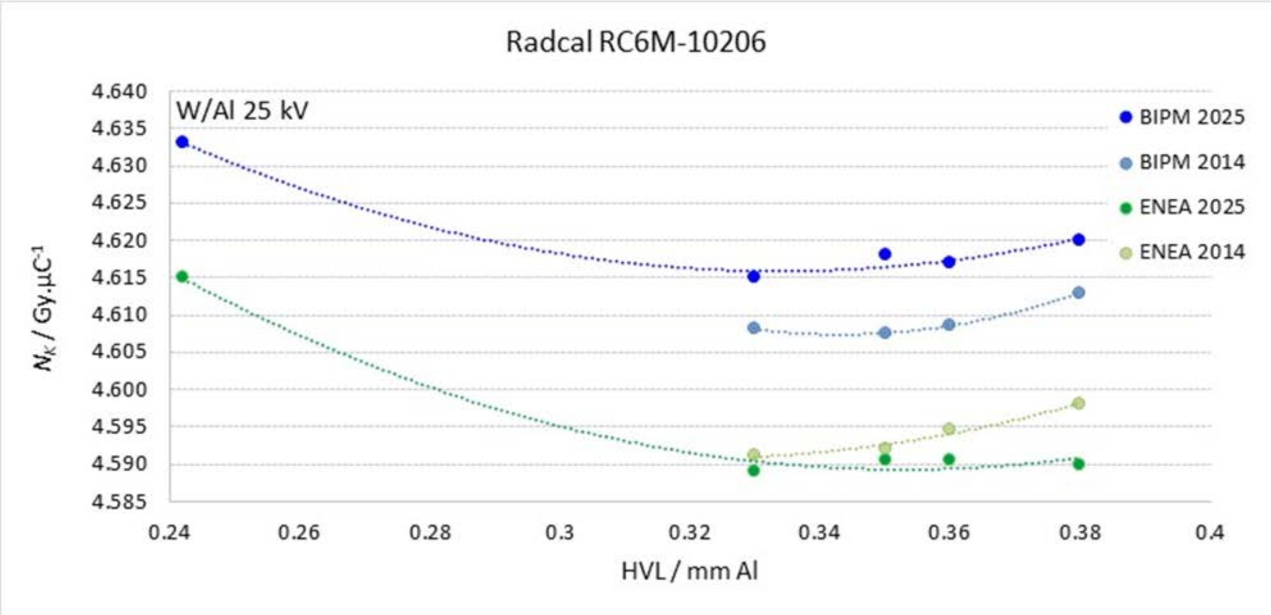

Figure 1. Calibration coefficients for the Radcal RC6M-10206 measured at the ENEA-INMRI and at the BIPM

This chamber was also used for the 2025 BIPM.RI(I)-K2 comparison run at the same time. The BIPM and ENEA-INMRI calibration coefficients corresponding to the radiation quality W/Al 25 kV are shown in Figure 1. The comparison result for the 25 kV W/Al is 0.9961, in very close agreement with the updated 2014 W/Mo results listed in Table 10, and consistent within the uncertainties with the present results.

Radcal RC6M chambers are known for their flat energy response in mammography beams. To study the energy dependence at the BIPM, the mammography results are usually normalized to the quality 25 kV W/Al, the closest W/Al x-ray quality in terms of HVL. Doing this analysis for this chamber, the energy dependence shows to be consistent with all the Radcal RC6M chambers calibrated at the BIPM, being the mean ratio $N_{K\_\mathrm{W/Mo}}$ / $N_{K\_\mathrm{25kV\_W/Al}}$ for this chamber 0.9967(4). Considering the ENEA-INMRI results, this ratio becomes 0.9946(2), indicating slightly greater energy dependence than that observed at the BIPM.

11. Degrees of Equivalence

The analysis of the results of BIPM comparisons in low-energy x-rays in terms of degrees of equivalence is described in Burns (2003) and a similar analysis is adopted for comparisons in mammography x-ray beams. Following a decision of the CCRI, the BIPM determination of the air-kerma rate is taken as the key comparison reference value, for each of the CCRI radiation qualities. It follows that for each laboratory i having a BIPM comparison result x_i with combined standard uncertainty u_i, the degree of equivalence with respect to the reference value is the relative difference $D_i = (\dot{K}_i - \dot{K}_{\mathrm{BIPM},i}) / \dot{K}_{\mathrm{BIPM},i} = x_i - 1$ and its expanded uncertainty $U_i = 2\,u_i$. The results for D_i and U_i, expressed in mGy/Gy and including those of the present comparison, are shown in Table 14 and in Figure 2.

12. Conclusions

The key comparison BIPM.RI(I)-K7 for the determination of air-kerma in mammography beams shows the standards of the ENEA-INMRI and the BIPM to agree at the level of the expanded uncertainty of the comparison of 7.8 parts in 10^3.

Tables and a graph of degrees of equivalence, including those for the ENEA-INMRI, are presented for entry in the BIPM key comparison database. Note that these data, while correct at the time of publication of the present report, become out of date as laboratories make new comparisons. In accordance with the validity rules for comparison data agreed by the CCRI(I), results older than 15 years are considered no longer valid and have been removed from the KCDB. The formal results under the CIPM MRA are those available in the key comparison database (KCDB 2026).

Table 14. Degrees of equivalence (Mo/Mo)

	Mo/Mo-25		Mo/Mo-28		Mo/Mo-30		Mo/Mo-35	
	D_i	U_i	D_i	U_i	D_i	U_i	D_i	U_i
	/(mGy/Gy)		/(mGy/Gy)		/(mGy/Gy)		/(mGy/Gy)	
VNIIM	**-3.7**	4.8	**-3.0**	4.8	**-2.7**	4.8	**-2.8**	4.8
VSL	**-5.6**	12.0	**-4.6**	12.0	**-5.3**	12.0	**-4.7**	12.0
BEV	**-4.0**	6.8	**-3.5**	6.8	**-3.5**	6.8	**-2.5**	6.8
CMI	**2.8**	7.0	**2.4**	7.0	**2.7**	7.0	**2.5**	7.0
KRISS	**-3.5**	4.0	**-3.6**	4.0	**-3.2**	4.0	**-3.7**	4.0
NIM	**0.1**	5.6	**-0.4**	5.6	**0.0**	5.6	**0.2**	5.6
NMIJ	**-5.5**	7.2	**-4.4**	7.2	**-4.8**	7.2	**-4.3**	7.2
PTB	**4.2**	7.2	**4.0**	7.2	**3.8**	7.2	**4.0**	7.2

Degrees of equivalence (W/Mo)

	W/Mo-23		W/Mo-25		W/Mo-28		W/Mo-30		W/Mo-35		W/Mo-50	
	D_i /(mGy/Gy)	U_i	D_i /(mGy/Gy)	U_i	D_i /(mGy/Gy)	U_i	D_i /(mGy/Gy)	U_i	D_i /(mGy/Gy)	U_i	D_i /(mGy/Gy)	U_i
NRC	**-0.7**	6.4					**-1.4**	6.4			**-2.1**	6.4
BFKH			**-0.7**	9.2			**-4.3**	9.2				
ENEA-INMRI	**-6.6**	7.8			**-6.8**	7.8	**-6.9**	7.8	**-7.8**	7.8		

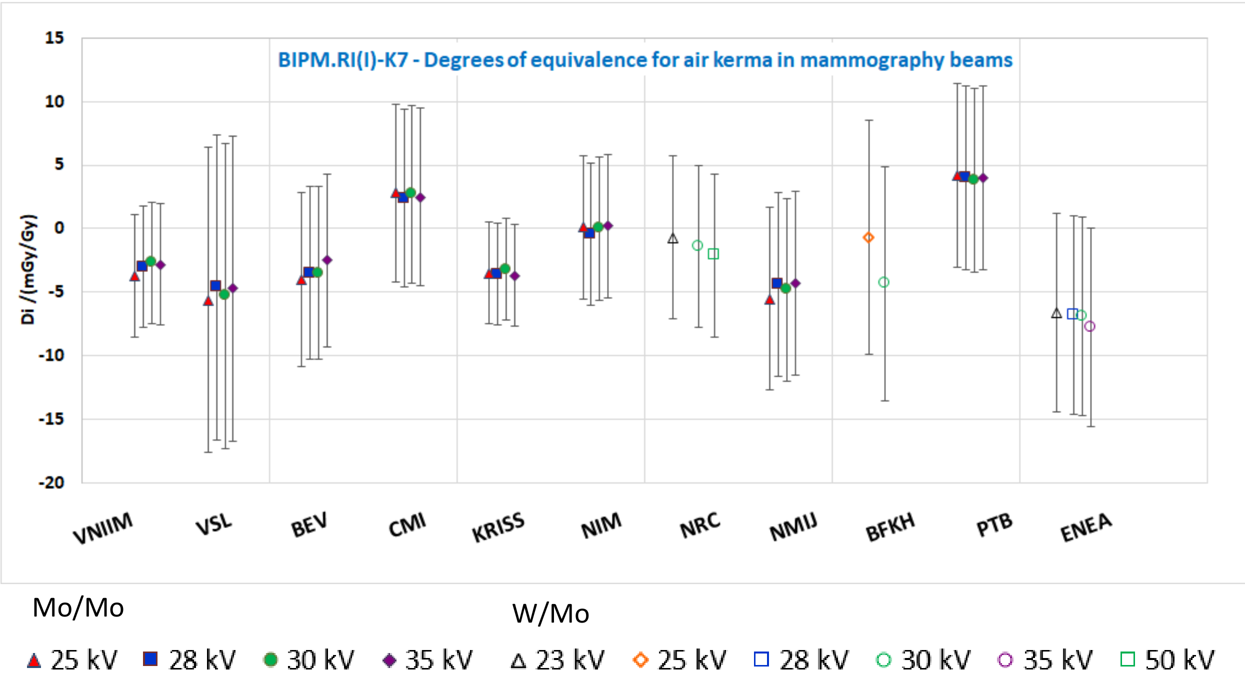

Figure 2. Graph of degrees of equivalence with the KCRV

References

Bielajew A F 1990 An analytic theory of the point-source nonuniformity correction factor for thick-walled ionisation chambers in photon beams *Phys Med Biol* **35** 517–538 (**DOI** 10.1088/0031-9155/35/4/004)

Boutillon M 1998 Volume recombination parameter in ionization chambers *Phys Med Biol* **43** 2061 (**DOI** 10.1088/0031-9155/43/8/005)

Boutillon M, Henry W H and Lamperti P J 1969 Comparison of exposure standards in the 10-50 kV x-ray region *Metrologia* **5** 1–11 (**DOI** 10.1088/0026-1394/5/1/002)

Burns D T 2003 Degrees of equivalence for the key comparison BIPM.RI(I)-K2 between national primary standards for low-energy x-rays *Metrologia* **40** 06031 (**DOI** 10.1088/0026-1394/40/1A/06031)

Burns D T 2004 Changes to the BIPM primary air-kerma standards for x-rays *Metrologia* **41** L3 (**DOI** 10.1088/0026-1394/41/1/L02)

Burns D T, Kessler C 2009 Diaphragm correction factors for free-air chamber standards for air-kerma in x-rays *Phys Med Biol* **54** 2737–45 (**DOI** 10.1088/0031-9155/54/9/009)

Burns D T, Kessler C 2018 Re-evaluation of the BIPM international dosimetry standards on adoption of the recommendations of ICRU Report 90 *Metrologia* **55** R21 (**DOI** 10.1088/1681-7575/aacb01)

Burns D T, Kessler C, Allisy P J 2009 Re-evaluation of the BIPM international standards for air-kerma in x-rays *Metrologia* **46** L21–23 (**DOI** 10.1088/0026-1394/46/5/N01)

ICRU 1979 Average energy required to produce an ion pair *J. ICRU* **os16** Issue 2 Report 31 (International Commission on Radiation Units and Measurements: Oxford University Press) (**DOI** 10.1093/jicru/os16.2.1)

ICRU 2016 Key data for ionizing-radiation dosimetry: Measurement standards and applications *J. ICRU* **14** Report 90 (International Commission on Radiation Units and Measurements: Oxford University Press)

KCDB 2026 Up-to-date results for comparison BIPM.RI(I)-K7 are available in the BIPM key comparison database at BIPM.RI(I)-K7

Kessler C 2006 Establishment of simulated mammography radiation qualities at the BIPM Rapport BIPM-2006/08

Kessler C, Burns D, Roger P, Toni M P, Pinto M, Bovi M, Cappadozzi G and Silvestri C 2015 Key comparison BIPM.RI(I)-K7 of the air-kerma standards of the ENEA-INMRI, Italy and the BIPM in mammography x-rays *Metrologia* **52** 06025 (**DOI** 10.1088/0026-1394/52/1A/06025)

Kessler C and Burns D T 2024 Measuring conditions and uncertainties for the comparison and calibration of national dosimetric standards at the BIPM *Rapport* BIPM-2024/04

Kondo S, Randolph M L 1960 Effect of Finite Size of Ionization Chambers on Measurements of Small Photon Sources *Radiation Research* **13** 37–60 (**DOI** 10.2307/3570872)

Laitano R, Pimpinella M and Toni M P 2005 Re-determination of the k_{sc}, k_e, k_{fl} correction factors for low and medium energy x-ray air-kerma measurement by the ENEA-INMRI free-air chambers CCRI(I)/05-32

Villevalde A, Burns D T and Kessler C 2020 Beam characterization for low-energy x-rays and new reference qualities at 1 m *Rapport* BIPM-2020/03